Drinking plastics? – Quantification and qualification of microplastics in drinking water distribution systems by µFTIR and Py-GCMS

Kirstein, Inga Vanessa; Hensel, Fides; Gomiero, Alessio; Iordachescu, Lucian; Vianello, Alvise; Wittgren, Hans B.; Vollertsen, Jes

Published in:
Water Research

DOI (link to publication from Publisher):
10.1016/j.watres.2020.116519

Publication date:
2021

Document Version
Publisher's PDF, also known as Version of record

Water Research 188 (2021) 116519

Contents lists available at ScienceDirect

Water Research

journal homepage: www.elsevier.com/locate/watres

Drinking plastics? – Quantification and qualification of microplastics in drinking water distribution systems by µFTIR and Py-GCMS

Inga V. Kirstein[a,*], Fides Hensel[a], Alessio Gomiero[b], Lucian Iordachescu[a], Alvise Vianello[a], Hans B. Wittgren[c], Jes Vollertsen[a]

[a] Aalborg University, Department of the Built Environment, Aalborg, Denmark
[b] NORCE Norwegian Research Centre AS, Norway
[c] Sweden Water Research /VA SYD, Sweden

ARTICLE INFO

Article history:
Received 23 July 2020
Revised 17 September 2020
Accepted 12 October 2020
Available online 13 October 2020

Keywords:
Small microplastic
Microplastic mass quantification
Drinking water treatment plants
Human health

ABSTRACT

While it seems indisputable that potable water contains microplastics (MP), the actual concentrations are much debated and reported numbers vary many orders of magnitude. It is difficult to pinpoint the cause of these differences, but it might be variation between waters, variation between quantification methods, and that some studies did not live up to rigorous analytical standards. Despite the urgent need to understand human exposure by drinking water, there is a lack of trustable methods generating reliable data. Essentially, proper MP assessment requires that quality assurance is in place and demonstrated, that an adequate volume of drinking water is assessed, and that differences in analytical methods are understood. This study presents a systematic and robust approach where MP down to 6.6 µm were assessed in potable water distribution systems in terms of quantity, size, shape, and material. For the first time, sub-samples were analysed by two of the most validated and complementary analytical techniques: µFTIR imaging and Py-GCMS. Both methods successfully determined low contents in drinking water. However, µFTIR and Py-GCMS identified different polymer types in samples with overall low MP content. With increasing concentration of a given polymer type, the values determined by the techniques became more comparable. Most detected MPs were smaller than 150 µm, and 32% were smaller than 20 µm. Our results indicate a potential annual uptake of less than one MP per person, suggesting that drinking potable water produced at a high-performance drinking water treatment plant represents a low risk for human health.

1. Introduction

We are living in the *Anthropocene* with all kind of plastic materials omnipresent in our daily life. The broad application of plastics in packaging technology, constructions, and other industries leads to a current global annual production of almost 360 million metric tons (PlasticsEurope, 2019). Due to their durability, most plastic types are poorly degradable, but rather become brittle over time and subsequently fractionate into ever-smaller pieces. The resulting microplastics (MPs) generally refer to plastic fragments ≤ 5 mm (Arthur et al., 2009; Barnes et al., 2009). Sub-categories differentiating between large MP (5 mm–500 µm) and small MP (500–1 µm) are frequently used (Primpke et al., 2020). During the past years, there has been a rapidly growing concern about MPs and researchers all over the globe started exploring their abundance, composition and morphology in various matrixes using different visual and analytical tools such as FTIR-, GCMS-, or Raman-based methods for MP identification. Hence, MPs have been reliably assessed in natural and anthropogenic environments (aquatic, terrestrial, and indoor and outdoor air) (Alimi et al., 2018; Horton et al., 2017; Vianello et al., 2019), but also in food, and drinking water, both bottled and tap water (Cox et al., 2019).

The omnipresence of plastics in all aspects of human life means that humans are inevitably exposed to MPs on a daily basis. It has been suggested that MPs enter the human gastro-intestine by the direct ingestion via, e.g. contaminated nourishment or beverages, causing a daily intake of MPs by the human body. Investigations of human stool showed that, at least partly, “what goes in, goes out” for MPs bigger than 50 µm (Schwabl et al., 2019). Nonetheless, the

* Corresponding author.
E-mail address: ivk@build.aau.dk (I.V. Kirstein).

https://doi.org/10.1016/j.watres.2020.116519

scientific community agrees that it becomes especially relevant to identify small (<500 µm) and very small (<20 μm) MPs, as MPs smaller than 500 μm have been suggested capable of passing the gut wall (Lusher et al., 2017) and MPs smaller than 20 µm have been demonstrated to accumulate in the liver, kidneys, and guts of mice (Deng et al., 2017).

Despite the implications for human health, limited research has been carried out on MPs in drinking water, and previous studies focused primarily on MPs in freshwater used for drinking water production rather than on the water directly consumed (Koelmans et al., 2019). Only a few studies focused on the quantification of MPs in bottled water (Mason et al., 2018; Oßmann et al., 2018; Schymanski et al., 2018) or potable water (Kosuth et al., 2018; Mintenig et al., 2019; Pivokonsky et al., 2018; Shruti et al., 2020). Additionally, the MP numbers reported in these studies vary by nearly 6 orders of magnitude, from 0.001 to 470 MPs/L (Kosuth et al., 2018; Mintenig et al., 2019; Pivokonsky et al., 2018; Shruti et al., 2020). Additionally, the authors sampled drinking water from different sources (ground- or surface water) in various countries and used different tools for MP identification, ranging from simple visual inspection to state-of-the-art µFTIR and micro-Raman analyses (Kosuth et al., 2018; Mintenig et al., 2019; Pivokonsky et al., 2018; Shruti et al., 2020). Hence, the discrepancy in findings points out the need for research on drinking water from different sources and countries, but also the comparison of different methods used for MP identification. As mentioned above, several methods are currently used for MP qualification and quantification, which makes a proper comparison of results throughout different studies challenging. The majority of published studies refer to MPs in terms of particle number within some size range (Löder et al., 2017). Such data is essential when assessing its environmental, ecological, or human health impacts, but insufficient when assessing the "MP concentration" in a respective matrix. Here, additionally, the mass of MPs must be quantified (Simon et al., 2018), representing a significant analytical problem as the spectroscopic based methods are well-suited for determination of chemical composition, size and shape, but less suited for quantification of mass (Liu et al., 2019). Thermoanalytical methods such as Pyrolysis-Gas Chromatography Mass Spectrometry (Py-GCMS) generally require larger particle masses compared to vibrational microscopy orientated methods. However, such an approach enables the characterisation of plastics' additives in the sample as well as the quantification of nanosized particles if an appropriate volume and an effective concentration step are considered.

Information on small and very small MPs is limited, and its consequences to human health are far from being understood. Hence, our primary focus was to strengthen the knowledge on MP quality and quantity, including very small MPs (<20 µm) in drinking water in terms of both mass and numbers. A further intention was to compare the MP mass assessment of FPA-µFTIR-Imaging and Py-GCMS in real potable water matrices. This combination of analytical approaches and this particular matrix is novel, and it is the ambition that it leads to an increased confidence in the obtained results, and the accuracy of both analytical techniques when assessing the content of small MPs in drinking water.

Starting at a Swedish high-performance drinking water treatment plant (DWTP), sampling locations were chosen along two drinking water distribution pipes of different age. The concentration, composition, size and morphology, as well as the related estimated mass of MPs was determined by µFTIR, and potential differences between pipe systems were assessed. The identification of MPs using µFTIR microscopy followed by an automated image analysis enabled us to quantify and qualify MP content and mass in each sample and to compare these data with MP concentrations determined via Py-GCMS. Recently, Koelmans et al. (2019) pointed out, that only four out of fifty reviewed studies on MPs in fresh-, drinking-, and wastewater scored positive on defined quality criteria, which were related to sampling, sample treatment, use of controls, analytical procedure, and polymer identification. In order to ensure and control the quality of our data, we: 1. analysed sample triplicates, and 2. analysed one blank per sampling location, 3. aimed for representative sample size, 4. followed highest standards during sampling, storage, and sample processing, and 5. assessed the full sample volume using the two complementary, reliable, and state-of-the-art polymer identification methods, namely µFTIR and Py-GCMS.

2. Materials and methods

2.1. Sampling strategy

The DWTP Sydvatten AB produces and supplies drinking water to 900,000 inhabitants in the south of Sweden (Skåne). The DWTP uses surface water originating from the lake Vombsjön for drinking water production. In general, drinking water production is based on artificial groundwater infiltration. Therefore, raw water seeps slowly through the alluvium of gravel and sand to natural groundwater storage. The so produced artificial groundwater is following pumped up and is initially aerated in order to remove iron and manganese and, following calcium ions are removed by the addition of sodium hydroxide. The resulting precipitate is removed by sedimentation. Next, chemical cleaning with a minor dosage of ferrous chloride takes place followed by sand bed filtration. Finally, the water is disinfected and pumped into the distribution network (Sydvatten, 2016). Sampling took place between May 13th and 16th 2019. Our goal was to follow treated drinking water produced and supplied by the DWTP Vombverket in order to cover variability in MP abundance of a similar source. Starting at Vombverket, we followed two supply pipelines 1. the pipe Vombverket (V) – Björnstorp (BJP) – Genarp (BJH), which was built in 2011, but first taken into use in 2018 and 2. the pipeline Vombverket (V) – Bonderup (BOP) – Genarp (BOH), which was built and used since 2000. The pipeline between Vombverket – Björnstorp – Genarp measures 3.9 km. The pipeline between Vombverket – Bonderup – Genarp measures 5 km. At both pipelines, samples were taken in parallel one day each, at a pumping station (sample sets BJP and BOP) and the corresponding hydrants (sample sets BJH and BOH) respectively.

At each station, triplicates of drinking water samples were filtered in parallel through 5 μm stainless steel filters (Haver & Boecker OHG, Germany), that were placed in custom modified stainless steel filter holders (Sterlitech Corporation, United States) attached via stainless steel pipes (Figure S1). The inlet tube was attached directly to a water tap at the pipe or to a hydrant. The water flow was adjusted to approximately 10 L min^{-1}. A flowmeter (Zenner International GmbH & Co. KG, Germany) was connected to each of the outlet tubes of the stainless steel filtration units to determine the volume of filtered water of each replicate.

At each sampling position, the complete setup was primed for ten minutes prior to applying filters. Between 200 and 1100 L of drinking water were filtered (Table S3). We aimed for 1 m^3 sample size, and the filtration was stopped earlier when stainless steel filters clogged, which led to a significant reduction of the water flow. After completion, the filters were transferred to muffled glass Petri dishes, covered with 70% ethanol and stored frozen at −20 °C until further processing.

2.2. Mitigating contamination

When working with samples produced for human consumption or where MP concentrations are expected to be low, it is of ut-

most importance to mitigate and control contamination. Therefore, the equipment used in our study was muffled at 500 °C or extensively rinsed with particle-free water (0.7 µm filtered) prior to use. All solutions used were filtered before trough a 0.7 µm glass fibre filter. In order to prevent airborne contamination, sample preparation was carried out in a laminar flow bench (Labogene, Scan-Laf Fortuna Clean Bench, Denmark) or in a lab equipped with a Dustbox® (Hochleitungsluftreiniger, Germany) unit with HEPA filter (H14, 7.5 m^2). Since contamination can never be completely excluded, one blank sample was taken at each station (Figure S1, Table S1), by using a cascade filtration consisting of a glass fibre (GF) filter of 0.7 µm pore size in front of the stainless steel filter. Furthermore, wet sedimentation traps loaded with 500 mL of 0.7 µm fibreglass filtered Milli Q water in the Py-GCMS room to QA/QC any contamination source during analysis. All blank samples were treated and analysed in parallel to the respective drinking water samples.

2.3. Extraction of microplastics

In the laboratory, samples were thawed and treated in "sets of stations" of three replicates each plus the respective blank sample under a laminar flow bench. The stainless steel filters were transferred into muffled glass beakers and incubated in 5% SDS for 24 h at 50 °C. Subsequently, filters were ultra-sonicated for five minutes (Elmasonic S50R, Germany). The filters were thoroughly flushed before being placed on a glass filtration unit. SDS was removed from the sample by flushing the beaker and the filtration unit intensively with particle-free Milli Q water and 50% ethanol. Subsequently, particles were flushed off the filters with particle-free 50% ethanol back into the beaker. Beakers were immediately covered with aluminium foil to prevent evaporation.

The sample set of BJP contained high amounts of inorganic particles which were removed performing a density separation using a sodium polytungstate (SPT) solution (TC-Tungsten Compounds, GmbH, Germany; $\rho = 1.8$ g cm^{-3}) in small glass separatory funnels by inflating air from the bottom and mixing the sample for 30 min. After a settling time of 24 h, the settled material was purged and the supernatant filtered on 5 µm stainless steel filter as described above.

The resulting particle-ethanol suspension was transferred gradually into a 10 mL muffled glass vial and evaporated by using a gentle flow of nitrogen gas at 50 °C (TurboVap, Biotage, Sweden). The final sample volume was adjusted to 5 mL. These sample-suspensions were ultra-sonicated (Elmasonic S50R, Germany) and homogenised before being transferred onto a zinc selenide transmission window. An aliquot, corresponding to 20 - 52% of the sample or blank sample (Table S3) was transferred onto the transmission window using glass capillary pipettes, covered and dried on a heating plate at 55 °C.

2.4. Analysis via µFTIR imaging

The abundance and chemical composition of the extracted MPs from drinking water was determined using a Focal Plane Array (FPA) – based Fourier Transformation Infrared Spectroscopy (FTIR) imaging technique. For this, a Cary 620 FTIR microscope coupled with a Cary 670 IR spectroscope (Agilent Technologies, USA) was used to scan the entire area of the enriched zinc selenide transmission windows (active diameter 10 mm, active area 78.5 mm^2). The microscope was equipped with a 25x Cassegrain objective producing 3.3 µm pixel resolution on a 128 × 128 mercury cadmium telluride (MCT) FPA detector. All scans were carried out in transmission mode with a spectral range of 3750 – 850 cm^{-1} at 8 cm^{-1} resolution applying 30 co-added scans in transmission mode. A background tile was collected before each sample's scan, using the same parameters but co-adding 120 scans instead of 30.

2.5. Analysis via Py-GCMS

After investigation via µFTIR, the remaining sub-samples were submitted to Py-GCMS analysis. The remaining aliquots of each of the ethanol/water suspended samples, ranging from 48 - 80% of the initial volume, were transferred onto a pre-muffled fibreglass filter (0.7 µm pore size) according to Gomiero et al. (2019). Filters were folded on pre-burnt pyrolysis cups and spiked with 10 µL of 25% tetramethylammonium hydroxide (TMAH) solution in water to derivatise the samples, hence allowing also the determination of previously polar and/or non-volatile compound. Pyrolysis cups were covered with a muffled glass beaker and dried on a heating plate at 30 °C overnight. Pyrolysis mass spectrometry analysis was performed following Gomiero et al. (2019). Eight amongst the most commonly used plastic polymers such as: polyethylene - PE, polypropylene - PP, polystyrene - PS, polyvinyl chloride - PVC, polyamide – PA 6,6; polymethyl methacrylate - PMMA, Polycarbonate - PC and polyethylene terphtalate - PET were investigated. Mass-based concentrations were calculated by fitting the obtained results onto calibration curves obtained by pyrolysing standard certified plastic polymers obtained from Goodfellow Ltd (Huntingdon, England). The limit of detection (LOD) was calculated according to Hermabessiere et al. (2018). Following, an evaluation of the signal to noise ratios (S/N) of the detected peaks at the lowest concentration levels in the calibration curves allowed the extrapolation to a 10:1 ratio pointing to the LOQ (Table S2). Obtained results are reported as µg of polymer type / L of sample.

2.6. Data handling, statistics and downstream analysis

The collected FPA-µFTIR-Imaging data were analysed using the software siMPle (Primpke et al., 2020) to automatically detect and quantify the particle content in each sample and blank sample, as well as measuring each particle's size and estimating its volume and mass. The size detection limit is defined by a combination of the filter size (5 µm) and the detection limit of the µFTIR. While the latter produced pixel sizes of 3.3 µm, a manual examination of the FTIR spectra showed that 'particles' represented by only 1 pixel on the FPA sometimes were false positives. When the particles comprised 2–3 pixels, the identification could be trusted. Therefore, the minimum particle size was set to three pixels, resulting in a minimum nominal size of 6.6 µm (i.e. a 'triangle' of pixels with a length and width of 2 pixels – 6.6 µm). To evaluate the quality and reliability of our data, we manually checked the respective spectra/reference of representative mapped minimum and maximum sized MPs of all detected polymer types (Figure S3).

The total amount of MPs per blank sample of each polymer type was subtracted from each sample of the respective sample set. As only whole particles exist, MP blank estimates have been rounded, and negative values were set to zero. For particle size analysis, non-corrected values were used.

Assuming an elliptical MP shape, the minor dimension was calculated from the major dimension, as the longest linear distance perpendicular to the major axis (Simon et al., 2018). To distinguish the MPs morphologically from each other, they were divided according to their dimensions into particles and fibres. An adjusted definition provided by the World Health Organization for the determination of airborne fibres was used, in which fibres are distinguished as objects with a length-width ratio of > 3 from particles with a ratio of ≤ 3 (Vianello et al., 2019).

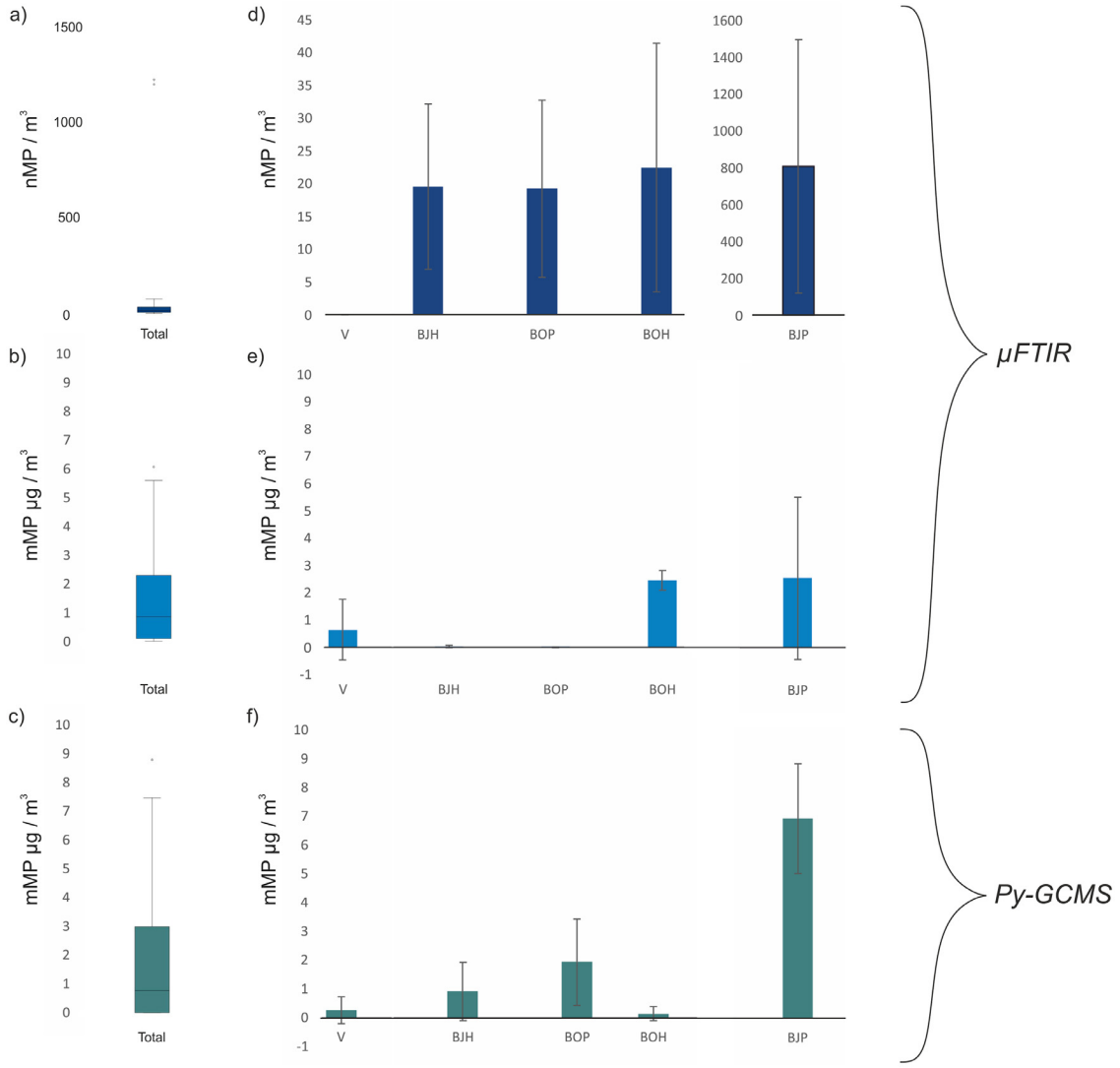

Fig. 1. Box Plot using blank corrected total (a) MP numbers, corresponding estimated (b) MP mass (n = 15) and, (c) mass concentration determined via Py-GCMS in the drinking water distribution system (n = 14). Blank corrected and averaged (n = 3) (d) MP numbers and (e) MP mass estimates based on µFTIR analysis as well as (f) mass estimates based on Py-GCMS, starting at the waterworks (V) following the two independent pipes (BOP-BOH and BJP-BJH).

In order to calculate MP mass, the particle volume was estimated by assuming that particles are ellipsoids. The third dimension was defined as 0.67 times the minor dimension, respectively. Consequently, the mass was estimated based on the resulting particle volume and the respective density of the polymer (Simon et al., 2018).

Univariate analyses were carried out with IBM SPSS statistics 25, while all multivariate analyses were carried out with the Primer 7 software package plus the add-on package PERMANOVA+ (PRIMER-ELtd, UK). Normality of the data was tested by a Shapiro-Wilk normality test. A non-parametric ANOVA Kruskal-Wallis test was used at a significance level of $p < 0.05$ to compare univariate groups. For multivariate analysis, MP numbers (nMP) and MP mass (mMP) were normalised by calculating their abundances per m^3. In order to cope with undefined resemblances, a dummy variable ($X + 1$) was added. Principal coordinates analysis (PCO) was performed using Bray-Curtis similarity on fourth root transformed data, to visualise patterns in polymer type composition. PERMANOVA with fixed factors and 9999 permutations at a significance level of $p < 0.05$ was performed to test for statistically significant variance amongst the polymer composition between sampling locations and age of the two pipelines.

3. Results

3.1. Monitoring contamination

In parallel to each sample set, one field blank was analysed to assess potential contamination. The degree of contamination was estimated as the number of MPs per blank sample and not the filtered water volume, as the contamination sources were related to sampling, processing, and analysis. We detected minimum MP contamination of 5 MPs/blank of the sample sets BJH and BOH, and maximum contamination of 155 MPs / blank of the sample set BOP. In general, we observed an average contamination of 46 ± 63 MPs / blank (n = 5). The polymeric composition of MPs detected in all blanks was 67% PE, 24% PA, 5% PET, 3% acrylic and 2% PP (Table S1).

3.2. Quantification of MPs in drinking water

Using state of the art FPA-µFTIR-Imaging, 9.4 million spectra were generated per sample scan. Combining FPA-µFTIR-Imaging with an automated particle detection produced in total 20 particle maps (triplicates plus one blank at five stations, respectively).

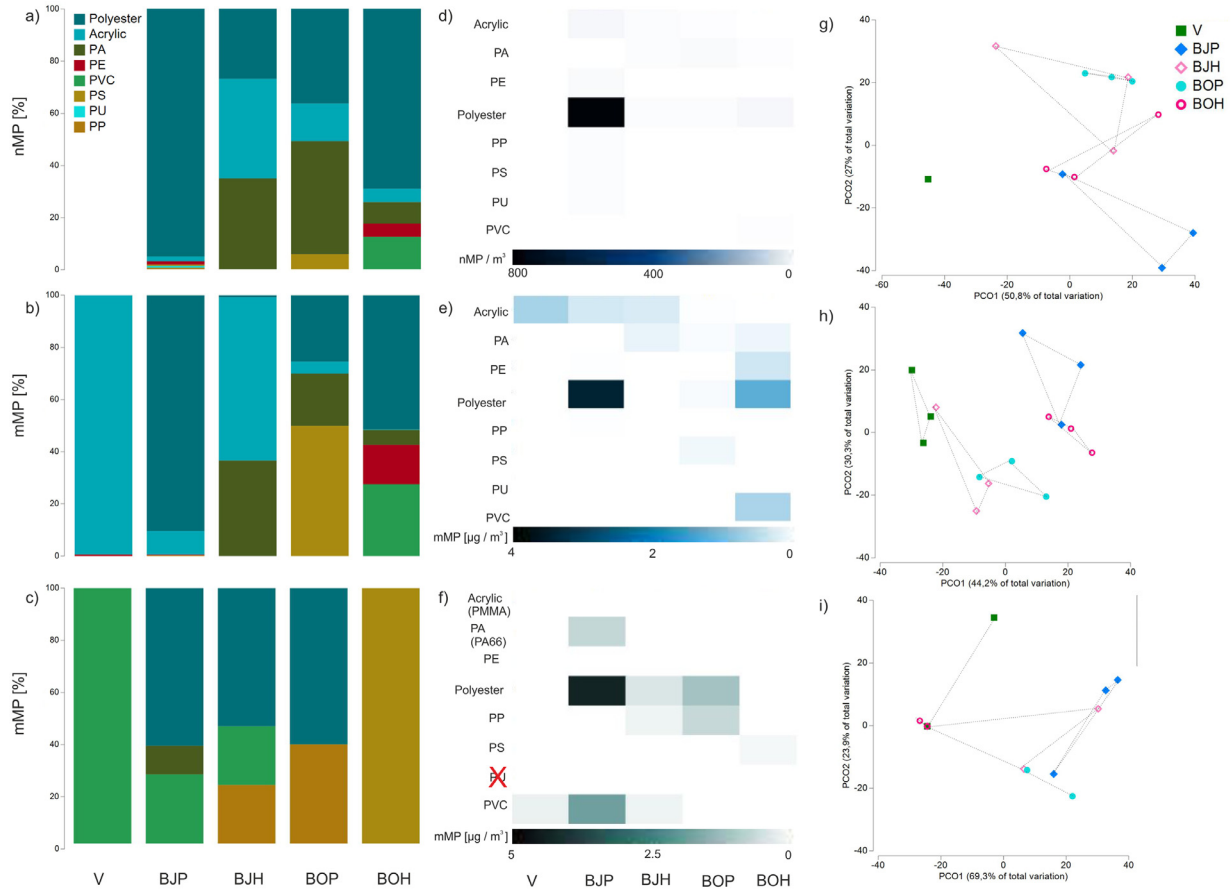

Fig. 2. Blank corrected and averaged (n = 3) relative abundances of MP (a) number, (b) mass estimates based on µFTIR analysis and (c) mass estimates based on Py-GCMS, starting at the waterworks (V) following the two independent pipes (BOP-BOH and BJP-BJH). Heat maps representing the relative abundance of the respective polymer types / m^3 determined via µFTIR (d, e) and Py-GCMS (f). Principle Coordinate Ordination for µFTIR-based (g) nMP, (h) nMP and Py-GCMS-based (i) mMP relating variation in the polymer composition between different sample sets. PCOs representing similarity of polymer composition based on fourth root transformed across samples. PA = polyamide, PVC = polyvinyl chloride, PS = polystyrene, PE = polyethylene, PU = polyurethane, PP = polypropylene.

The presence of MPs was evaluated by the Pearson's correlation of each map pixel to a custom-built spectral database (Figure S2, S3), containing more than 100 reference spectra (Liu et al., 2019). All samples revealed the presence of MPs (Figure S4). However, after blank correction, samples from the waterworks (V) were emended to zero (Fig. 1, S5).

The average number of MPs/m^3 detected in the whole drinking water distribution system within the week of sampling was, 174 ± 405 MPs/m^3. It ranged from a minimum of zero MPs/m^3 at the waterworks (samples V_S1 - V_S3), to a maximum of 1219 MPs/m^3 in one sample from the pumping station BJP (Fig. 1a, c, Table S3).

Generally, the highest MP numbers have been detected in the sample set BJP with an average of 809 ± 688 MPs / m^3 (Fig. 1a, Table S3). In contrast, in samples from BJH, BOP, and BOH similar numbers of 20 ± 13, 19 ± 14, 22 ± 19 MP/m^3 were estimated, respectively (Fig. 1a, Table S3).

MP mass estimates reflect a completely different picture, e.g., even though no nMP were estimated in the blank-corrected samples from the waterworks (V), these showed positive mass estimates. Vice versa, sample sets BJH and BOP with moderate nMP estimates showed very low mMP estimates of 4 and 29 ng/m^3, respectively. This effect is the result of higher/lower mass estimates of MPs in the blank sample of the respective sample set (Fig. 1e, Table S3).

In order to further assess MP mass concentration, sub-samples were analysed by Py-GCMS, enabling us to compare µFTIR-based mass-estimates and Py-GCMS mass-based determination of mMP. We successfully measured very low concentrations with the two complementary techniques for MP analysis. Furthermore, the estimated and determined mass concentrations were of the same order of magnitude throughout all drinking water samples and, the highest mass concentration was estimated and determined for the same sample set BJP (Fig. 1, Table S3, S4).

In order to test if the pipe age (8 vs. 19 years) had a significant effect on nMP and mMP, a Kruskal-Wallis test was conducted. Comparing samples from the two pipelines (n = 12) revealed no significant differences with respect to this parameter, neither for nMP nor for estimated or determined mMP ($p > 0.05$) (Table S5).

3.3. MP composition in drinking water

Microplastics identified in drinking water samples via µFTIR were assigned to eight different polymer groups (Fig. 2a, b). Except for sample set V, nMP and mMP polymer composition of drinking water generally appeared heterogenic within and between various sample sets (Fig. 2, S1). With reference to µFTIR quantification of nMP, the sample sets BJP and BOH were clearly dominated by polyester, whereas the sample set BJH and BOP showed a high proportion of polyamide (PA) (Fig. 2). Generally, the highest abundances in single samples were recognised for PA (0–100%), followed by polyester (0–100%), and acrylic (0–29%) (Figure S4). Furthermore, the sample BOH_S2 was dominated by PVC (50%), and the sample BOP_S3 consisted of a high proportion of PS (29%). The

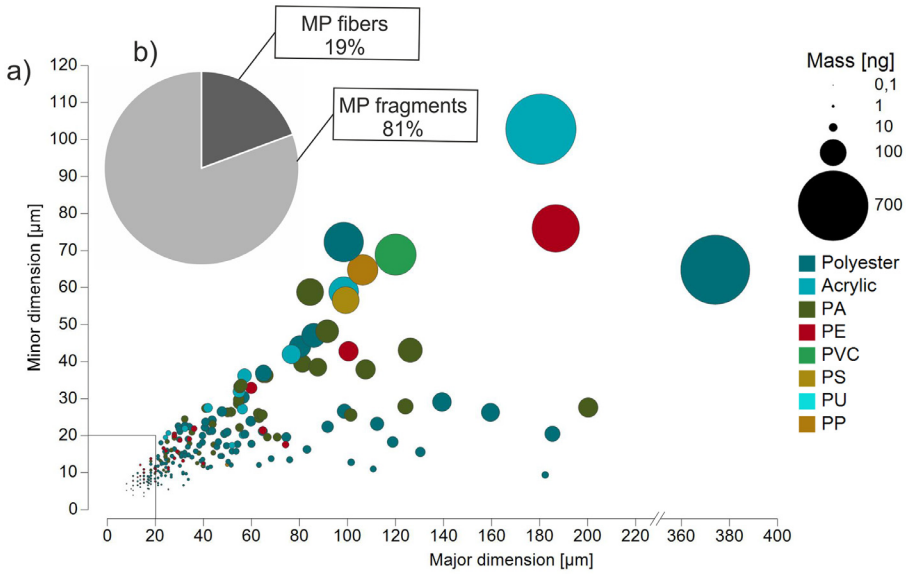

Fig. 3. (a) Bubble plot representing minor vs major dimension of all detected MP in the drinking water distribution system (n = 15). Various polymer types are indicated by different colours. Mass estimates of respective MP are indicated by bubble size. Black squares indicate size range of < 20 µm in both major and minor dimension. (b) Percentage of MP fibres and fragments for the total analysed samples. The threshold for fibre classification was a length-width ratio of > 3.

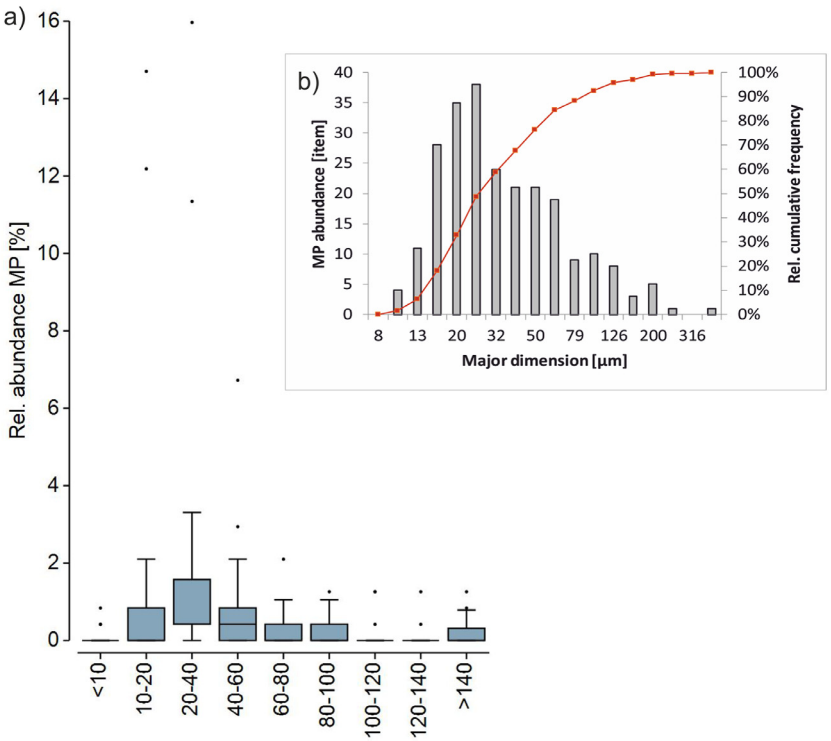

Fig. 4. MP size considering particle's major dimension. (a) Box-and-whiskers plot of MP relative abundances in different size classes from all drinking water samples. The upper and lower boundaries of the box indicate the 75th and 25th percentiles, respectively. The line within the box marks the median, error bars indicate the 90th and 10th percentiles, and black dots represent outliers. (b) Size distribution for the total amount of MP particles identified in all analysed samples for major dimension. Bin intervals were selected as 0.1 on a logarithmic scale. Bars on the histograms indicate abundance; the red dotted line is the relative cumulative frequency (secondary axis).

other polymers occurred in clearly lower proportions, namely PE, PU, and PP (Fig. 2, S1).

Using Py-GCMS, we reliably identified five out of the eight µFTIR identified polymer groups across all samples (Fig. 2c). Polyethylene, PU, and acrylic compounds were not detected or below the detection limit. The polymer composition ranged from one to maximum of three polymer groups within sample sets (Fig. 2c). Sample set V and BOH consisted solely of PVC and PS, respectively. All three sample sets BJP, BJH, and BOP were dominated by polyester. Additionally, samples of BJP consisted of PVC and PA, samples of BJH consisted of PVC and PP, and samples of BOP consisted of PP.

Comparing mMP, µFTIR-estimated and Py-GCMS-determined plastic types per m^3 revealed that the abundance of most plastic types appeared rather random when MP numbers/concentrations were low (Fig. 2d, e, f). Vice versa, when MP numbers increase,

the same increase could be observed in estimated and determined mass as, e.g., for polyester at station BJP (Fig. 2d, e, f).

The polymer composition of the various samples was compared using Principle Coordinate Ordination (PCO) to determine whether nMP or mMP sample sets were distinct from each other (Fig. 2g, h, i). Samples of different stations were not clearly divided, neither for nMP nor for µFTIR-based or Py-GCMS-based mMP with the first two axes representing more than 70% of the total variation within the analysed samples in all three cases (Fig. 2g, h, i). However, PERMANOVA revealed that there were significant differences between stations in all three cases ($p < 0.05$) (Table S6). A separate test of dispersion using PERMDISP revealed that these differences amongst sample sets were not driven by within-system heterogeneities (Table S6). Since sample replication ($n = 3$) did not allow to obtain a significant result on the level $p = 0.05$, pairwise tests between stations were not carried out. Comparing samples taken at the two different pipe systems revealed no significant differences with respect to pipe age (8 vs. 19 years) neither for nMP nor for mMP ($p > 0.05$) (Table S6).

3.4. Size and shape of MPs in drinking water

To characterise size and shape of detected MPs, major and minor dimensions were evaluated. Considering both major and minor dimension, we found that 32% of all MPs detected were < 20 µm (Fig. 3). According to the threshold used for fibre classification (length-width ratio of > 3), 46 out of 238 (19%) of all detected MPs were fibres. Hence, the remaining 81% were defined as particles (Fig. 3b). The identified fibres composition was dominated by polyester (87%), followed by PE (9%) and a single PP fibre. The biggest MP was detected in a sample of BOH with 374 µm in major and 76 µm in minor dimension and consisted of polyester (PET). The smallest MP detected had a major dimension of 8 µm and minor dimension of 5.2 µm and was assigned to a polyester particle (PET) in sample BJP_S1 (Fig. 3a, Figure S3).

A Shapiro-Wilk test revealed that neither major nor minor dimension of the overall detected MPs were normal distributed ($p < 0.05$). Hence, we used median values (D50) to describe our data (Table S7). Overall, the size distribution of all identified MPs (Fig. 4) had D50s of 26 µm and 13 µm for the major and minor dimension, respectively (Table S7). Table S7 comprises the D10, D50, and D90 values for individual sampling sites. Considering only particles major dimension, the size of MPs detected ranged between 8 and 374 µm (Fig. 4).

4. Discussion

4.1. MPs in drinking water – quantity and quality

The primary goal of our study was to strengthen the knowledge on MP quality and quantity, including very small MPs (< 20 µm), in drinking water. Through the combination of representative sample size, quality control and assurance together with state-of-the-art µFTIR imaging and Py-GCMS, MPs could be qualified and quantified in all analysed drinking water of the investigated distribution system. Average MPs concentrations were generally low (between zero and 0.022 ± 0.019 MPs/L) except one pumping station which had considerably higher MPs numbers (0.809 ± 0.688 MPs/L). Hence, our results are within the range of MP numbers reported by other studies (Kosuth et al., 2018; Mintenig et al., 2019; Pivokonsky et al., 2018; Shruti et al., 2020). Comparable to our study, Mintenig et al. (2019) reported low MP numbers in drinking water (0.001 MPs/L) using a µFTIR approach. This aspect contrasts with the studies by Pivokonsky et al. (2018), Kosuth et al. (2018), and Shruti et al. (2020) which reported substantially higher MP numbers (6, 18, and 470 MPs/L, respectively). It is important to note that these three studies only analysed small sample volumes (0.5 - 1 L), and used either a visual staining-based approach or Micro-Raman spectroscopy, making a comparison with our data hardly possible.

For MPs, identification via μFTIR imaging has proven efficient (Bergmann et al., 2019; Liu et al., 2019; Mintenig et al., 2019; Simon et al., 2018). This technique allows scanning of large areas of filters or windows for the presence of MP and has been successfully applied down to 10 μm MP particles. In the present study, we further decreased this size limit by applying a 25x Cassegrain objective producing 3.3 µm pixel resolution, which allowed us to determine particles down to 6.6 µm. This imaging technique also allows the automatisation of MP identification and has been proven as a reliable tool for MP analysis (Primpke et al., 2020, 2019). While single-point FTIR or Raman spectroscopy for the larger particles and μFTIR or µRaman imaging spectroscopy for the smaller particles allow high-quality microplastic quantification, the techniques are time-consuming and require advanced analytical equipment. Pyrolysis GC–MS (Hendrickson et al., 2018; Gomiero et al., 2019; Fischer et al., 2019) and thermal desorption GC–MS (Dümichen et al., 2015; 2019) is also an option for determining the polymer composition of the particles which has received increased attention. For screening purposes where estimates suffice, simple techniques such as chemical staining have been suggested and applied to some matrices (Shim et al., 2016; Maes et al., 2017). However, there still are many unanswered questions, here amongst which plastic types this approach can target, how applicable the approach is on complex matrixes, and whether or not it is faster than the FTIR based techniques.

Microplastics can enter freshwater environments in various ways. They can originate from degraded plastic waste, industrial effluents, surface run-off and wastewater effluents, but also from sewer overflows and atmospheric deposition (Horton et al., 2017; Müller et al., 2020). In this context, drinking water treatment processes are essential to ensure adequate water quality, but they are not completely efficient in removing MPs, as MP removal ranges between 70% and 82% (Pivokonsky et al., 2018). Beside incomplete removal during water purification, the deterioration of plastic equipment used during water purification or distribution is likely a source for MPs in drinking water, as pipes in DWTPs are frequently made of PVC, PP, and PE (Mintenig et al., 2019). In the present study, surface water served as source for drinking water production. Since the raw water was not investigated, we cannot evaluate the MP removal efficiency of the DWTP. Nevertheless, since MPs are generally in lower concentrations than in raw waters (Pivokonsky et al., 2018), the low MP concentrations we found at the high-performance DWTP and most of the following distribution system point towards a successful MP removal during drinking water treatment. Further investigations are needed in order to assess how MPs concentrations in potable water can be influenced by pre-treatment methods in DWP and the corresponding economic levels, in particular raw water sources.

Here, we also assessed the potential differences in MP loads between two distribution pipes of different age (8 vs. 19 years). The investigated distribution pipes mainly consist of cement, stainless steel, cast iron, and PE. Considering the low numbers of PE detected in the samples, it can be concluded that ten years' age difference had no significant impact on the MP loads in the distribution system. This finding is supported due to the fact that water is generally not reactive with PE and that 50 to 100-year service of PE potable water pipes used for pressurised, cold and/or hot water were projected (Whelton et al., 2009). However, the investigated sampling locations differed significantly in their polymer composition. In total, we identified eight different polymer types, including PA, polyester, acrylic, PVC, PS, PE, PU, and PP in drinking water throughout all samples. Previously anal-

ysed drinking water samples mainly contained polyester, PVC, PE, PA, and PP particles (Kosuth et al., 2018; Mintenig et al., 2019; Shruti et al., 2020). In the present study, polyester MP numbers were significantly higher at one pumping station (BJP). In contrast, Mintenig et al. (2019) reported no differences in MP numbers or composition at different stages of the distribution system (waterworks vs household). Generally, airborne contamination is a likely source for polyester. However, given the low numbers of polyester in the blank samples, contamination of our samples with polyester during sampling or processing is unlikely. The high polyester loads were determined in the lowest sample volume, which resulted from filter clogging by fine particulate matter. Neither at the DWTP, before the distribution system, nor at the respective hydrant such high MP abundances were recognised. Hence, our findings suggest a short term weakness/damage in the pipeline at the time of sampling, presumably due to construction work or the like.

4.2. MPs in drinking water – numbers matter, but mass matters too

The few existing studies that quantified MPs in drinking water report numbers that vary by several orders of magnitude (Kosuth et al., 2018; Mintenig et al., 2019; Pivokonsky et al., 2018; Shruti et al., 2020). This discrepancy indicates high variability of MP loads in drinking waters from different sources and countries. However, the studies are also hardly comparable due to different sampling, MP extraction, and identification methods, where MP identification represents one of the crucial pitfalls (Käppler et al., 2018). Furthermore, MP numbers are commonly reported within size classes (Löder et al., 2017) impeding the assessment of the "real" MP concentration and making it impossible to compare the data to analytical techniques quantifying the polymer mass. Previous work has demonstrated that both, ATR-FTIR and Py-GCMS successfully differentiate between plastic and non-plastic (Hendrickson et al., 2018; Käppler et al., 2018) with identification of 85% as the same polymer type (Käppler et al., 2018). For the first time, we analysed sub-samples via µFTIR imaging and Py-GCMS in order to compare MP concentrations, FTIR-based mass estimates, and directly determined mass concentrations. We successfully determined very low MP loads in drinking water, applying two µFTIR and Py-GCMS and obtaining comparable concentrations with the two complementary techniques. However, µFTIR and Py-GCMS identified different polymer types in samples with overall low MP concentrations, as i.e., PE was detected by µFTIR but not by Py-GCMS. Conversely, with increasing MP load of a given polymer type, the concentrations measured with both techniques became more comparable, as was the case for polyester. Underrepresentation of specific plastic types, due to concentrations below the respective polymer detection limit of Py-GCMS, is the most likely explanation for the differences in polymer composition observed between the different methods.

4.3. MPs in drinking water – implications for human health

Using µFTIR imaging followed by an automated image analysis enabled us to identify the size and shape of MPs down to 6.6 μm. Since accessible clean drinking water is one of the Sustainable Development Goals of the United Nations (WHO, 2017), it is of utmost importance to reliably investigate MPs and to determine numbers, concentration, and size, in order to understand and evaluate the potential risks related to human health. Considering that the annual estimated MP consumption ranges from 39,000 to 52,000 particles or 74,000 and 121,000 when inhalation is taken into account (Cox et al., 2019), the generally low MP numbers of 0.174 MPs/L we found in the present study suggest that the consumption of drinking water, processed by a high-performance drinking water treatment plant, does not particularly add to potential risks to human health.

However, the issue of MPs in products designated for human consumption received increasing attention in the last years due to the discovery of small MPs translocating to inner organs (Deng et al., 2017). In the present study, MP abundance increased with decreasing size (until 20–40 µm), before decreasing to the smallest detectable size (<10 µm). The latter aspect is a consequence of the low spectra quality (S/N ratio) when size decreases below 10 µm, resulting in fewer particles positively identified as a specific polymer and/or nonsysthetic particle. Pivokonsky et al. (2018) found MPs were the most abundant in the smallest detectable size class (1–10 μm), accounting for up to 95% of the total numbers. Also, Shruti et al. (2020) reported an increase in MPs with decreasing size, with 50% of MPs < 500 µm. Unfortunately, the different methodologies applied in the previous study makes the comparison hardly feasible. The fact that we exclusively detected MPs between 8 and 374 µm, and that 32% of all detected MPs were smaller than 20 µm, may raise concern for human health. Investigations of MPs in fish and invertebrates suggest that MPs smaller than 500 μm might pass the gut wall (Lusher et al., 2017), and MPs smaller than 20 µm can accumulate in liver, kidney and gut of mice (Deng et al., 2017). However, the European Food Safety Authority (EFSA) classified the absorption of MPs larger than 150 µm as unlikely, and the absorption and uptake of MPs smaller than 20 µm (in total up to 0.3% for MPs < 150 µm) into organs as overall limited (EFSA, 2016). In order to put our results in perspective, approximately 97% of the MPs we detected were smaller than 150 µm in major dimension and MP numbers were on average 0.174 MPs/L. Considering a scenario with MP absorption of 0.3% and daily consumption of three litres potable water per day, the annual uptake would be of less than one MP particle per person through drinking potable water. Hence, to support a more robust human health risk assessment of MPs, future efforts need to be done to understand better the occurrence of plastic particles in potable water, their levels as number of particles and total masses, polymer type composition, size and shape. The latter features are of crucial importance for toxicologists to define exposure routes and tailor natural like exposure scenario to investigate realistic biological effects and define toxicity thresholds.

5. Conclusion

This study represents a systematic and robust approach investigating MP quality, quantity, shape, and size, including very small MPs (< 20 µm), in drinking water. As such, it is an important step forward in understanding MP distribution and the potential implications for human health. Most detected MPs were smaller than 150 µm, and 32% were smaller than 20 µm, which could potentially pose a risk to human health. However, our results showed very low MP loads in drinking water processed in a high-performance drinking water treatment plant, suggesting a low risk to human health. For the first time, we investigated MP loads in drinking water using two complementary techniques, µFTIR imaging and Py-GCMS, and successfully determined very low MP loads in comparable concentrations.

Declaration of Competing Interest

The authors declare that they have no known competing financial interests or personal relationships that could have appeared to influence the work reported in this paper.

Acknowledgements

We like to thank the staff of the water utilities Sydvatten and VA SYD for organisational and technical support during the sampling campaign. Especially, we would like to thank Britt-Marie Pott and Magnus Ek for all their help and organisational support. Furthermore, we would like to thank Kjell Birger Øysæd (NORCE) for technical assistance during chemical analysis via Py-GCMS. This work was supported by Svenskt Vatten Utveckling (Project 18–112) and by Sweden Water Research.

Supplementary materials

Supplementary material associated with this article can be found, in the online version, at doi:10.1016/j.watres.2020.116519.

References

Alimi, O.S., Farner Budarz, J., Hernandez, L.M., Tufenkji, N., 2018. Microplastics and nanoplastics in aquatic environments: aggregation, deposition, and enhanced contaminant transport. Environ. Sci. Technol. 52, 1704–1724.

Arthur, C., Baker, J.E., Bamford, H.A., 2009. Proceedings of the International Research Workshop on the Occurrence, Effects, and Fate of Microplastic Marine Debris, September 9-11, 2008. University of Washington Tacoma, Tacoma, WA, USA.

Barnes, D.K., Galgani, F., Thompson, R.C., Barlaz, M., 2009. Accumulation and fragmentation of plastic debris in global environments. Philosophical transactions of the Royal Society of London. Series B. Biol. Sci. 364, 1985–1998.

Bergmann, M., Mützel, S., Primpke, S., Tekman, M.B., Trachsel, J., Gerdts, G., 2019. White and wonderful? Microplastics prevail in snow from the Alps to the Arctic. Sci. Adv. 5 eaax1157.

Cox, K.D., Covernton, G.A., Davies, H.L., Dower, J.F., Juanes, F., Dudas, S.E., 2019. Human consumption of microplastics. Environ. Sci. Technol. 53, 7068–7074.

Deng, Y., Zhang, Y., Lemos, B., Ren, H., 2017. Tissue accumulation of microplastics in mice and biomarker responses suggest widespread health risks of exposure. Sci. Rep. 7, 46687.

EFSA, 2016. Statement on the presence of microplastics and nanoplastics in food, with particular focus on seafood. EFSA J. 30 (EFSA Panel on Contaminants in the Food Chain)pp.

Gomiero, A., Øysæd, K.B., Agustsson, T., van Hoytema, N., van Thiel, T., Grati, F., 2019. First record of characterization, concentration and distribution of microplastics in coastal sediments of an urban fjord in south west Norway using a thermal degradation method. Chemosphere 227, 705–714.

Hendrickson, E., Minor, E.C., Schreiner, K., 2018. Microplastic abundance and composition in western Lake Superior as determined via microscopy, Pyr-GC/MS, and FTIR. Environ. Sci. Technol. 52, 1787–1796.

Hermabessiere, L., Himber, C., Boricaud, B., Kazour, M., Amara, R., Cassone, A.-.L., Laurentie, M., Paul-Pont, I., Soudant, P., Dehaut, A., Duflos, G., 2018. Optimization, performance, and application of a pyrolysis-GC/MS method for the identification of microplastics. Anal. Bioanal. Chem. 410, 6663–6676.

Horton, A.A., Walton, A., Spurgeon, D.J., Lahive, E., Svendsen, C., 2017. Microplastics in freshwater and terrestrial environments: evaluating the current understanding to identify the knowledge gaps and future research priorities. Sci. Total Environ. 586, 127–141.

Koelmans, A.A., Nor, N.H.M., Hermsen, E., Kooi, M., Mintenig, S.M., De France, J., 2019. Microplastics in freshwaters and drinking water: critical review and assessment of data quality. Water Res. 155, 410–422.

Kosuth, M., Mason, S.A., Wattenberg, E.V., 2018. Anthropogenic contamination of tap water, beer, and sea salt. PLoS One 13, e0194970.

Käppler, A., Fischer, M., Scholz-Böttcher, B.M., Oberbeckmann, S., Labrenz, M., Fischer, D., Eichhorn, K.-J., Voit, B., 2018. Comparison of μ-ATR-FTIR spectroscopy and py-GCMS as identification tools for microplastic particles and fibers isolated from river sediments. Anal. Bioanal. Chem. 410, 5313–5327.

Liu, F., Olesen, K.B., Borregaard, A.R., Vollertsen, J., 2019. Microplastics in urban and highway stormwater retention ponds. Sci. Total Environ. 671, 992–1000.

Lusher, A., Welden, N., Sobral, P., Cole, M., 2017. Sampling, isolating and identifying microplastics ingested by fish and invertebrates. Anal. Methods 9, 1346–1360.

Löder, M.G., Imhof, H.K., Ladehoff, M., Löschel, L.A., Lorenz, C., Mintenig, S., Piehl, S., Primpke, S., Schrank, I., Laforsch, C., 2017. Enzymatic purification of microplastics in environmental samples. Environ. Sci. Technol. 51, 14283–14292.

Mason, S.A., Welch, V.G., Neratko, J., 2018. Synthetic polymer contamination in bottled water. Front. Chem. 6, 407.

Mintenig, S., Löder, M., Primpke, S., Gerdts, G., 2019. Low numbers of microplastics detected in drinking water from ground water sources. Sci. Total Environ. 648, 631–635.

Müller, A., Österlund, H., Marsalek, J., Viklander, M., 2020. The pollution conveyed by urban runoff: a review of sources. Sci. Total Environ. 709, 136125.

Oßmann, B.E., Sarau, G., Holtmannspötter, H., Pischetsrieder, M., Christiansen, S.H., Dicke, W., 2018. Small-sized microplastics and pigmented particles in bottled mineral water. Water Res. 141, 307–316.

Pivokonsky, M., Cermakova, L., Novotna, K., Peer, P., Cajthaml, T., Janda, V., 2018. Occurrence of microplastics in raw and treated drinking water. Sci. Total Environ. 643, 1644–1651.

PlasticsEurope, 2019. Plastics - the facts 2019 - An analysis of European plastics production, demand and waste data.

Primpke, S., Cross, R.K., Mintenig, S.M., Simon, M., Vianello, A., Gerdts, G., Vollertsen, J., 2020. EXPRESS: toward the systematic identification of microplastics in the environment: evaluation of a new independent software tool (siMPle) for spectroscopic analysis. Appl. Spectrosc., 0003702820917760.

Primpke, S., Dias, P., Gerdts, G., 2019. Automated identification and quantification of microfibres and microplastics. Anal. Methods 11, 2138–2147.

Schwabl, P., Köppel, S., Königshofer, P., Bucsics, T., Trauner, M., Reiberger, T., Liebmann, B., 2019. Detection of various microplastics in human stool: a prospective case series. Ann. Intern. Med. 171, 453–457.

Schymanski, D., Goldbeck, C., Humpf, H.-.U., Fürst, P., 2018. Analysis of microplastics in water by micro-Raman spectroscopy: release of plastic particles from different packaging into mineral water. Water Res. 129, 154–162.

Shruti, V., Pérez-Guevara, F., Kutralam-Muniasamy, G., 2020. Metro station free drinking water fountain-A potential "microplastics hotspot" for human consumption. Environ. Pollut. 261, 114227.

Simon, M., van Alst, N., Vollertsen, J., 2018. Quantification of microplastic mass and removal rates at wastewater treatment plants applying Focal Plane Array (FPA)-based Fourier Transform Infrared (FT-IR) imaging. Water Res. 142, 1–9.

Sydvatten, 2016. Sydvatten – collaborating for public welfare [www document]. https://sydvatten.se/wp-content/uploads/2016/02/Sydvatten-in-English.pdf

Vianello, A., Jensen, R.L., Liu, L., Vollertsen, J., 2019. Simulating human exposure to indoor airborne microplastics using a breathing thermal manikin. Sci. Rep. 9, 1–11.

Whelton, A.J., Dietrich, A.M., 2009. Critical considerations for the accelerated ageing of high-density polyethylene potable water materials. Polym. Degrad. Stab. 94, 1163–1175.

WHO, W.H.O., 2017. Progress on drinking water, sanitation and hygiene: 2017 update and SDG baselines.